INL/RPT-24-77853

# High-Fidelity Neutronics Model of a Realistic Heat Pipe Microreactor Report

May 2024

Stefano Terlizzi[1], Ishita Trivedi[1], and Ryan Stewart[1]

[1]*Idaho National Laboratory*

Idaho National Laboratory

*INL is a U.S. Department of Energy National Laboratory operated by Batelle Energy Alliance, LLC*

INL/RPT-24-77853

# High-Fidelity Neutronics Model of a Realistic Heat Pipe Microreactor Report

**Stefano Terlizzi**[1]**, Ishita Trivedi**[1]**, and Ryan Stewart**[1]

[1]**Idaho National Laboratory**

**May 2024**

**Idaho National Laboratory**
**Nuclear Science and Technology**
**Idaho Falls, Idaho 83415**

**http://www.inl.gov**

**Prepared for the**
**U.S. Department of Energy**
**Office of Nuclear Energy**
**Under DOE Idaho Operations Office**
**Contract DE-AC07-05ID14517**

*Page intentionally left blank*

# SUMMARY

This report details the development of a high-fidelity reactor physics model of a generic heat-pipe-cooled microreactor (HPMR) —in the neutronics code Serpent—, named the realistic heat-pipe-cooled microreactor (rHPMR). The model covers the neutronic characteristics including cycle length, reactivity feedback, and neutron spectrum. The rHPMR provides a generic model that researchers can utilize to make safeguards considerations without disclosing proprietary information. In addition to this, we describe a Python wrapper which automates the generation of Serpent inputs of the rHPMR for the purpose of simulating misuse and diversion scenarios. This wrapper is used to model and simulate a case of fuel misuse and diversion. The rHPMR benchmark is used to exercise the computational tools which will be utilized later for the analysis of the Nuclear Test Reactor (NTR).

Negotiations are currently underway between Westinghouse and INL to obtain design information for the NTR. Once the negotiations have been completed, a separate report will be delivered to detail the neutronics characteristics of the NTR.

## ACKNOWLEDGEMENTS

This research made use of the resources provided by the U.S. Department of Energy National Nuclear Security Administration along with contributions from the U.S. Department of Energy Microreactor Program and of the resources of Idaho National Laboratory's High Performance Computing systems located at the Collaborative Computing Center and supported by the Office of Nuclear Energy of the U.S. Department of Energy and the Nuclear Science User Facilities under Contract No. DE-AC07-05ID14517.

The first author would like to acknowledge the contribution of Mustafa Jaradat, Namjae Choi, and Vincent Laboure from Idaho National Laboratory for their insights on the realistic heat-pipe-cooled microreactor design. Specific contributions from the authors are detailed below:

1. Stefano Terlizzi—Conceptualization, development of the realistic heat-pipe-cooled microreactor design, neutronic analysis, formal analysis, investigation, writing, reviewing & editing, visualization, supervision

2. Ishita Trivedi—Conceptualization, Python wrapper development, reviewing & editing

3. Ryan Stewart—Conceptualization, writing, reviewing & editing, supervision, funding acquisition, .

*Page intentionally left blank*

# CONTENTS

SUMMARY .......... iii

ACKNOWLEDGMENT .......... iv

1 INTRODUCTION .......... 1

2 The Realistic Heat-Pipe-Cooled Microreactor .......... 2

3 CODES AND WORKFLOW .......... 4

4 NUMERICAL RESULTS .......... 6

4.1 Neutronic Characterization .......... 6

4.2 Simulating Core Deviations with PyRATES .......... 8

5 DEVELOPMENT OF PRELIMINARY ACQUISITION PATHWAYS .......... 13

6 SUMMARY AND FUTURE WORK .......... 14

REFERENCES .......... 16

# FIGURES

Figure 1. Serpent-generated (a) radial view, (b) axial view, and (c) zoom-in of rHPMR fuel compacts. .......... 3
Figure 2. Representative submodules developed within PyRATES utilizing *sea-serpent* submodule. .......... 5
Figure 3. Spectrum per unit lethargy at BOL and EOL. .......... 7
Figure 4. Effective multiplication factor vs. time for the rHPMR at 1000 K. Error bars indicate three-sigma uncertainty. .......... 9
Figure 5. rHPMR radial core layout showing the manipulated fuel assembly indicated with a red hexagon. Five fuel compacts were replaced with the dummy case composition shown in Table 5. .......... 10
Figure 6. Effective multiplication factor vs. time for the rHPMR at 1000 K for a nominal (blue) and diversion scenario (red). Error bars indicate three-sigma uncertainty. ... 11
Figure 7. Fission source (warm colors) and thermal flux (cool colors) distributions for nominal and diversion scenarios for rHPMR. .......... 12

# TABLES

Table 1. Geometrical specifications of the rHPMR. Linear dimensions in centimeters and angular dimensions in degrees. .... 4
Table 2. Geometrical and material specifications for TRISO particles. .... 4
Table 3. Temperature reactivity feedback coefficient for the rHPMR at BOL. .... 8
Table 4. Kinetics parameters for the rHPMR. .... 8
Table 5. Modifications in TRISO fuel kernel composition to simulate diversion case. .... 10
Table 6. Multiplication factor comparison between nominal and diversion scenario. .... 10
Table 7. Expected parameters of importance related to the high-fidelity neutronics model. The first column provides model parameters that can be perturbed. The second column describes how the model parameter would affect core operations. The third column provides a list of expected detectable signals that would be effected... 14

# ACRONYMS

| | |
|---|---|
| **APA** | acquisition pathway analysis |
| **BOL** | beginning-of-life |
| **CRAB** | Comprehensive Reactor Analysis Bundle |
| **DOME** | Demonstration and Operation of Microreactor Experiments |
| **DT** | digital twin |
| **EOL** | end-of-life |
| **HPMR** | heat-pipe-cooled microreactor |
| **INL** | Idaho National Laboratory |
| **MR** | microreactor |
| **NTR** | Nuclear Test Reactor |
| **rHPMR** | realistic heat-pipe-cooled microreactor |
| **SFM** | special fissionable material |
| **TRISO** | TRi-structural ISOtropic |

*Page intentionally left blank*

# 1. INTRODUCTION

A microreactor (MR) is characterized by compactness, portability, and low power output. These features enable MRs to supply electricity, and eventually process heat, to remote areas. They also allow MRs to be integrated into small grids, such as on islands or in disaster impacted areas. While there are benefits to MRs, their compact size, portability, scalability, and lifetime create challenges for the traditional safeguard approaches that are tailored for large-scale stationary light-water reactors.

Westinghouse is planning to deploy a prototypic eVinci$^{TM}$ microreactor, called the Nuclear Test Reactor (NTR), at the Idaho National Laboratory (INL) Demonstration and Operation of Microreactor Experiments (DOME) facility by the beginning of 2026 [1]. In Fiscal Year 2024, a new National Nuclear Security Administration (NNSA)–funded project was started to create a digital twin (DT) of the NTR. This DT will the be used to perform predictive analyses of the NTR. Additionally, the DT will be leveraged to perform acquisition pathway analysis (APA). APA will help determine how significant quantities of special fissionable material (SFM) can be obtained from MRs and to test new safeguard mechanisms specific for MRs.

This report has two main purposes. First, it details the neutronic characteristics of a realistic heat-pipe-cooled microreactor (rHPMR). The rHPMR was created to be representative a TRi-structural ISOtropic (TRISO) fueled heat-pipe-cooled microreactor (HPMR), including the eVinci$^{TM}$-like NTR. The rHPMR will be used to test the computational tools that will be utilized to analyze the NTR once design specifications become available. Second, we describe a Python interface that we developed to generate Serpent inputs representing different configurations of the rHPMR corresponding to misuse and diversion scenarios.

The remainder of this report is structured as follows. Section 2 describes the rHPMR model geometry and material characteristics. Section 3 describes the codes used for the analysis and Python wrapper. Section 4 contains results for the neutronic Monte Carlo model, including the beginning-of-life (BOL), end-of-life (EOL), and a simplified diversion and misuse scenario. Section 5 highlights how the neutronics is expected to be used to perform APA. A summary and future work are finally addressed in Section 6.

This work does not include a detailed analysis of the NTR. Negotiations are currently underway between Westinghouse and INL to obtain design information for the NTR; once the negotiations have been completed, a separate report will be delivered to detail the neutronics characteristics.

## 2. The Realistic Heat-Pipe-Cooled Microreactor

The rHPMR is a 5-$MW_{th}$ reactor developed to preserve key neutronic characteristics, including expected burnup levels, fuel form, and relative importance of the temperature reactivity coefficients of the envisioned eVinci$^{TM}$ and NTR without releasing proprietary information. The rHPMR was originally created for a work sponsored by the DOE Microreactor program to perform mechanistic source term calculations through the combined use of the Comprehensive Reactor Analysis Bundle (CRAB) and MELCOR [2]. This work has leveraged and adapted the design described in Reference [3]. Leveraging the previous work allows the team to focus on developing the core of the rHPMR to examine APA, rather than duplicating work. To this extent, the original rHPMR has been modified to allow for material replacement and core alterations sufficient to describe material diversion or misuse.The rHPMR is a proxy of the NTR that is going to be placed in the INL DOME facility.

A radial and axial view of the core mid-plane is shown in Figure 1. From Figure 1.a, it is noticeable that the core contains 18 hexagonal assemblies arranged into two rings. Each assembly contains 72 cylindrical fuel “pins” (comprised of stacked fuel compacts) and heat pipes drilled into a graphite monolith. Six fuel pins surround each heat pipe to allow for adequate cooling. The fuel compacts contain TRISO particles dispersed in a graphite matrix with a packing fraction of 36% and enrichment of 19.78 wt%. The TRISO particles, explicitly modeled in Serpent and visible in Figure 1.b, have the dimensions and composition of the fuel tested within the Advanced Gas Reactor-2 (AGR-2) campaign with $UO_2$ kernels [4]. The top and bottom surface of the 160-cm-high assemblies are surrounded by 20-cm-high axial beryllium reflectors. The fuel compacts, heat pipes, and monolith are radially surrounded by a 0.05 cm gap. The gaps are added to accommodate for thermal expansion and fission gas release. The core is surrounded by 12 control drums, employing boron carbide as the neutron absorber.

The reactor’s geometrical specifications are reported in Tables 1; Table 2 reports the material constituting each TRISO layer and the corresponding mass density. The reactor is expected to have a lifetime of 4 to 5 years at full power that is equivalent to a burnup of 21.76 MWd/kgU. The burnup was chosen to be representative of the envisioned burnup level for the eVinci$^{TM}$ reactor according to open literature [5].

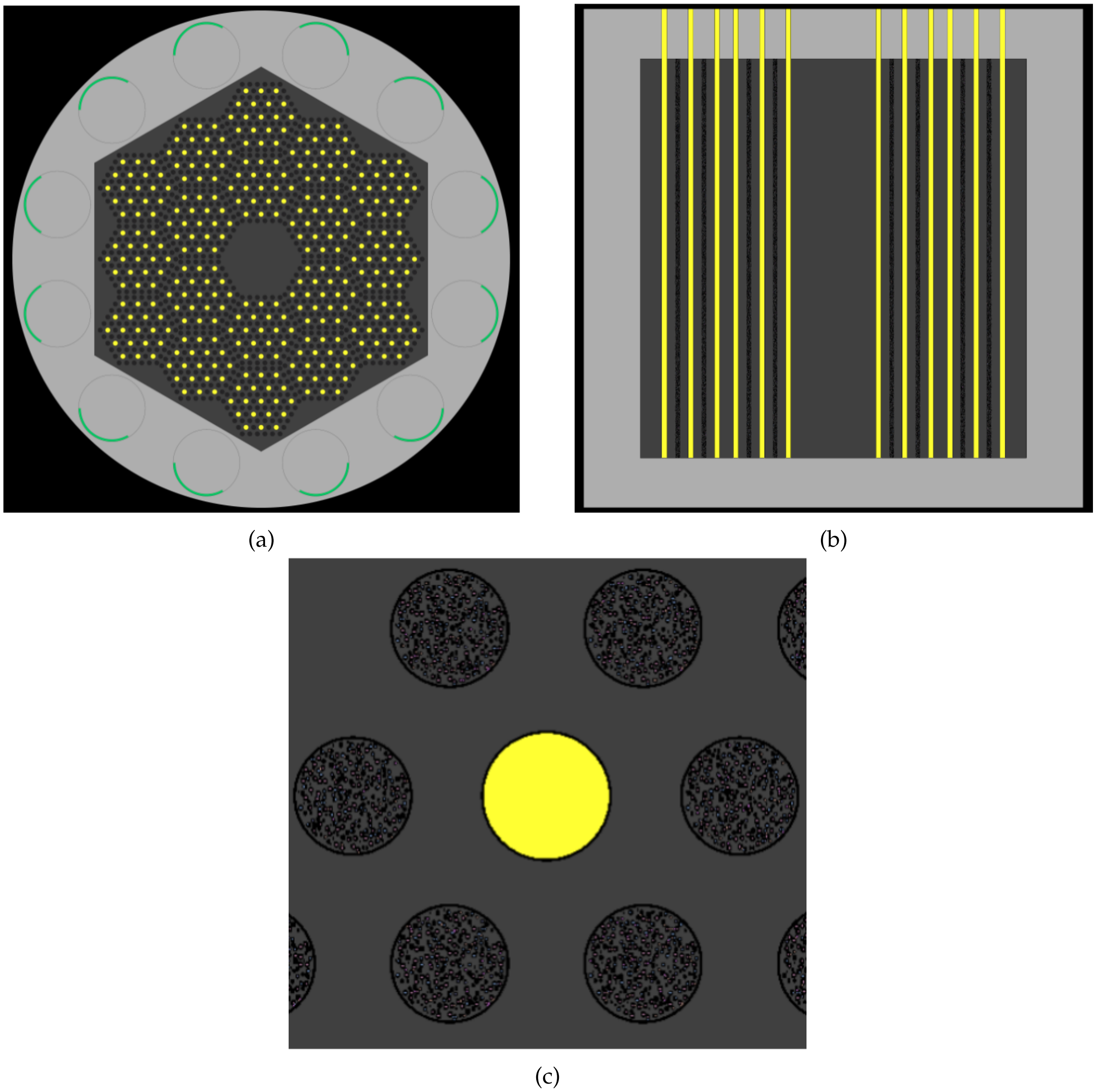

Figure 1: Serpent-generated (a) radial view, (b) axial view, and (c) zoom-in of rHPMR fuel compacts.

Table 1: Geometrical specifications of the rHPMR. Linear dimensions in centimeters and angular dimensions in degrees.

| **Property** | **Value** |
|---|---|
| Fuel Radius | 1.0 |
| TRISO Packing Fraction | 36% |
| Fuel Compact Gap | 0.05 |
| Heat Pipe External Radius | 1.1 |
| Heat Pipe Gap | 0.05 |
| Pin Pitch | 3.4 |
| Assembly Pitch | 32.0 |
| Monolith Apothem | 75.0 |
| Gap Around Monolith | 0.05 |
| Distance of Drums from Core Center | 95.0 |
| Poison Strip Internal Radius | 14.0 |
| Control Drum External Radius | 15.0 |
| Arc Width for Poison Strip | 120.0 |
| Gap Around Control Drums | 0.05 |
| Reactor External Radius | 112.0 |
| Active Zone Height | 160.0 |
| Top Reflector Thickness | 20.0 |
| Bottom Reflector Thickness | 20.0 |

Table 2: Geometrical and material specifications for TRISO particles.

| Component | Thickness $\mu m$ | Material | Density $g/cm^3$ |
|---|---|---|---|
| Kernel | 250 | $UO_2$ | 10.4 |
| Buffer | 100 | Graphite | 1.0 |
| IPyC | 40 | Pyrolitic Carbon | 1.9 |
| SiC | 35 | SiC | 3.2 |
| OPyC | 40 | Pyrolitic Carbon | 1.9 |

## 3. CODES AND WORKFLOW

A Python interface, called the Python Reactor Analysis Toolkit for Engineering Simulations (PyRATES), was implemented to automate the generation of Serpent inputs simulating misuse and diversion scenarios. Figure 2 provides a high level overview of the PyRATES module and sub-modules facilitating the creation and analysis of Serpent models for different kinds of reactors. Some of the reactor specific sub-modules developed within PyRATES are shown in Figure 2. The *sea_serpent* submodule is intended as a base submodule containing a conglomeration of methods to generate basic surfaces, cells, universes, materials, and detector creation for nuclear reactors. Other submodules such as *kugelpy* and *agn* have been used in previous research [6, 7].

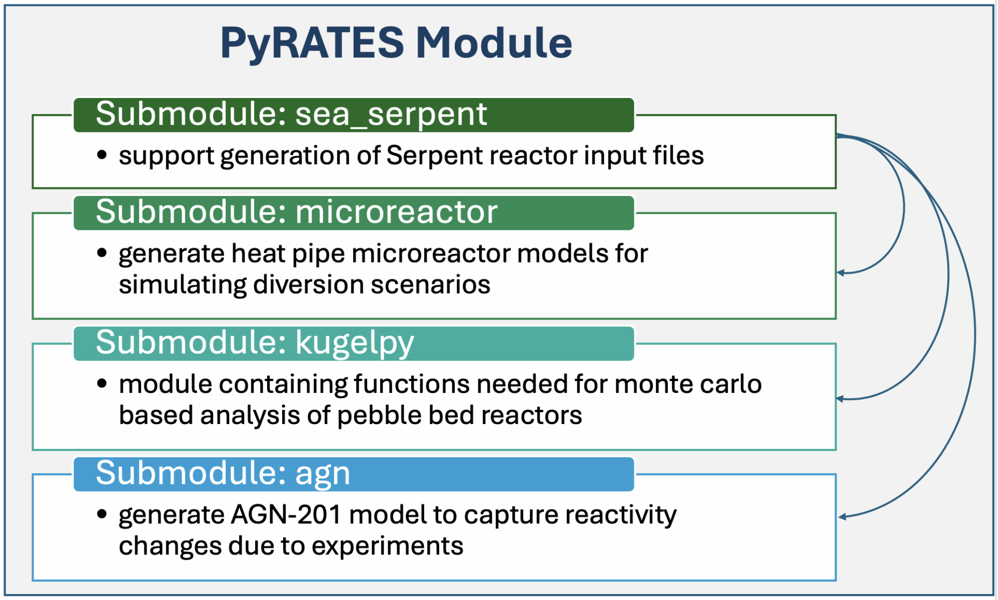


Figure 2: Representative submodules developed within PyRATES utilizing *sea-serpent* submodule.

The *microreactor* submodule was developed for this work to generate different configurations of a HPMR. This will be used for both the rHPMR and the NTR. The *microreactor* submodule allows an exploration of various diversion and misuse scenarios with relative ease and facilitates reproducible models where a user can adjust core components for a given safeguards scenario. For example, an entire fuel pin or a number of fuel compacts can be removed and replaced with a different material to simulate either diversion, if a non-fertile material replaced the fuel, or misuse, if depleted uranium replaced the fuel. Additionally, users can replace individual compacts from various fuel assemblies to reduce reactivity penalties associated with removing fuel.

Built into the *microreactor* module is the ability to adjust control drum angles. This provides the user additional means for masking potential diversion scenarios. For example, if fuel was removed from an outer edge, the control drum could be adjusted to try and match the nominal core.

Currently being developed in this system is the ability to "tally" various physical quantities, which may be of interest for detecting diversion or misuse. Tallies in Monte Carlo neutronics codes allow sampling of various physical phenomena, such as the neutron flux, fission rate, etc. A goal of this project is to determine what sensors (i.e., tallies) will be necessary to quantify diversion or misuse in the core. The *microreactor* module will provide users with an interface for determining which physical quantities should be monitored.

# 4. NUMERICAL RESULTS

This section contains selected results concerning the characterization of the rHPMR neutronic response. The results concern both the BOL and EOL are reported in Section 4.1. An application of the *microreactor* submodule applied to simulating a scenario of misuse and diversion of nuclear fuel from the rHPMR is presented in Section 4.2.

## 4.1 Neutronic Characterization

The neutronics studies contained in this section were conducted with Serpent (v. 2.2). This continuous energy Monte Carlo code was chosen due to its efficiency for problems characterized by a high number of surfaces thanks to the Woodcock tracking algorithm implemented within [8, 9]. All the simulations leverage the ENDF/B-VIII.0 continuous energy library [10] and are performed with 1,000,000 particles per cycle for 600 cycles (of which 100 are inactive). The statistics were chosen to obtain an uncertainty below 10 pcm in the effective multiplication factor. The depletion calculation were performed by defining three axial zones and two radial depletion zones for the reactor. The depletion analysis is performed by burning only the fuel that is the major contributor to the spectral changes in the reactor. Future work will investigate the effect of burning the boron carbide absorber on the reactivity and lifetime of the reactor.

The rHPMR neutron spectrum per unit lethargy is shown in Figure 3. It is noticeable that the reactor exhibits a thermal spectrum with the neutron spectrum hardening from BOL to EOL. The thermal spectrum is due to the large quantity of graphite and beryllium in the reactor that lead to high levels of neutron thermalization.

The temperature reactivity feedback coefficients and kinetic parameters, which include the delayed neutron fraction and generation time, were calculated to characterize the reactor's behavior during transient and depletion scenarios. The fuel temperature reactivity coefficient and the isothermal temperature reactivity coefficient, denoted by $\alpha_{T_f}$ and $\alpha_{T_t}$, respectively, are reported in

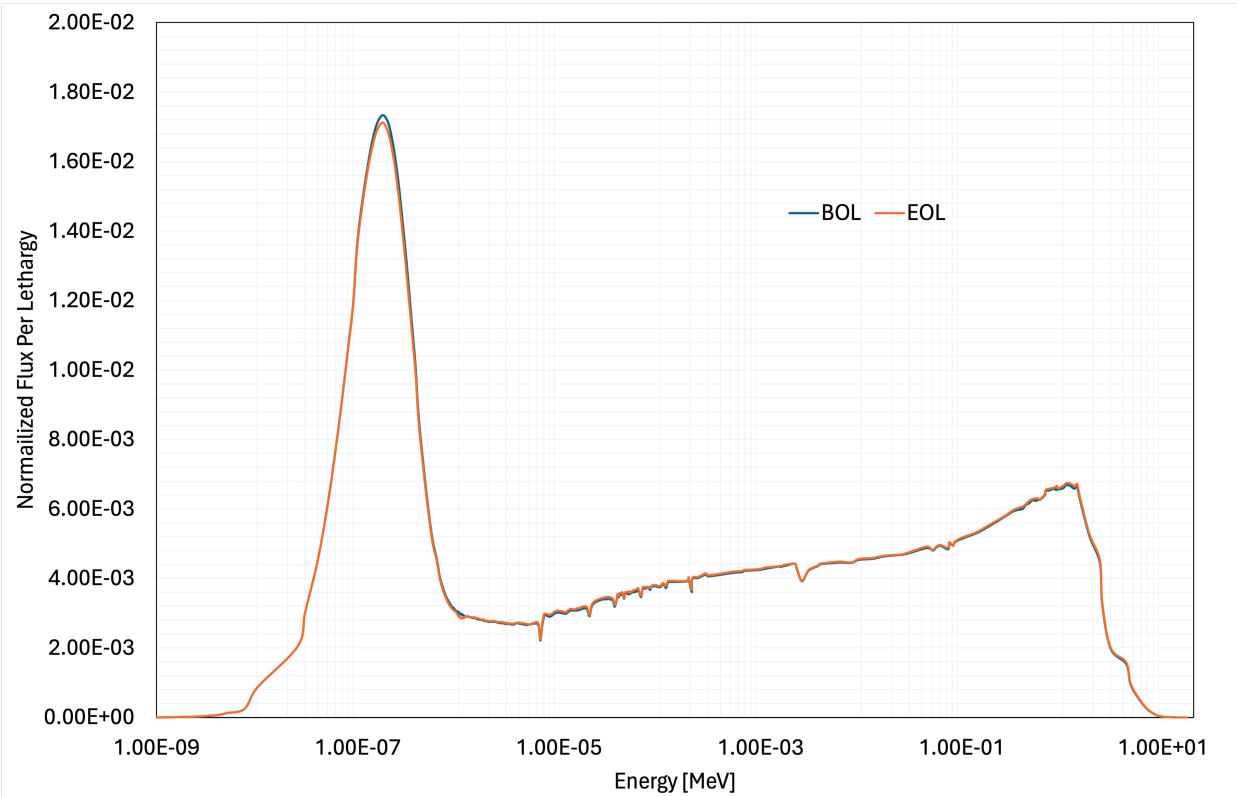


Figure 3: Spectrum per unit lethargy at BOL and EOL.

Table 3 and computed with the following equation:

$$\alpha_{T_x} = \left( \frac{1}{k_{eff}(1000)} - \frac{1}{k_{eff}(1200)} \right) \frac{10^5}{200K}, \tag{1}$$

where $k_{eff}(1000)$ and $k_{eff}(1200)$ denote the value of the effective multiplication factor for the temperature of the material of interest at 1000 and 1200 K, respectively. From Table 3, the dominant temperature feedback mechanism for the rHPMR is the fuel Doppler reactivity contribution, denoted by $\alpha_{Tf}$, that ensures the controllability of the reactor together with the graphite monolith reactivity coefficient, $\alpha_{Tm}$. On the contrary, the reflector reactivity coefficient, $\alpha_{Tr}$, is positive. However, this contribution is one order of magnitude lower that the fuel Doppler reactivity coefficient, therefore leading to a global negative temperature response. For the sake of completeness, the total control drums reactivity worth, denoted with $\alpha_\theta$, is also reported for BOL, demonstrating the ability to shut down the reactor at BOL. The control drum worth will be imperative to understanding changes in reactor operations over time, as the control drums will move over time at different rates corresponding to the amount of SFM present.

Table 3: Temperature reactivity feedback coefficient for the rHPMR at BOL.

| Feedback Coefficient | Value |
|---|---|
| $\alpha_{T_f}$, pcm/K | -4.59 |
| $\alpha_{Tm}$, pcm/K | -2.21 |
| $\alpha_{Tr}$, pcm/K | 0.17 |
| $\alpha_{\theta}$, pcm | 13,173 |

The kinetic parameters are reported in Table 4 at both BOL and EOL. The results are obtained for hot conditions that correspond to the reactor at an isothermal temperature of 1100 K.

Table 4: Kinetics parameters for the rHPMR.

| Kinetics Parameter | BOL | EOL |
|---|---|---|
| $\Lambda$ (s) | 1.95734E-04 | 2.08552E-04 |
| $\beta$ | 6.63907E-03 | 6.10275E-03 |
| $\beta_1$ | 2.90591E-04 | 2.52542E-04 |
| $\beta_2$ | 1.12869E-03 | 9.12939E-04 |
| $\beta_3$ | 1.16402E-03 | 1.11457E-03 |
| $\beta_4$ | 2.69454E-03 | 2.46706E-03 |
| $\beta_5$ | 9.20043E-04 | 1.00877E-03 |
| $\beta_6$ | 4.41185E-04 | 3.46871E-04 |

Figure 4 illustrates the effective multiplication factor plotted as a function of time, revealing that the reactor remains supercritical throughout its entire operational history. The results are obtained by depleting the core at nominal power (i.e., 5 $MW_{th}$) for the whole lifetime, with control drums fully withdrawn. An operating temperature of 1000 K was imposed throughout the simulation. From Figure 4, the letdown curve exhibits a classical trend where the effective multiplication factor decreases as a function of time. In particular, we notice the familiar dip due to xenon buildup in the first day of operation followed by a linear decrease due to the lack of burnable absorbers and the lack of the depletion of the boron carbide absorber.

## 4.2 Simulating Core Deviations with PyRATES

To demonstrate the use of PyRATES for effectively simulating diversion test cases, two models of the rHPMR core were generated with PyRATES. The first model is the base case equivalent to

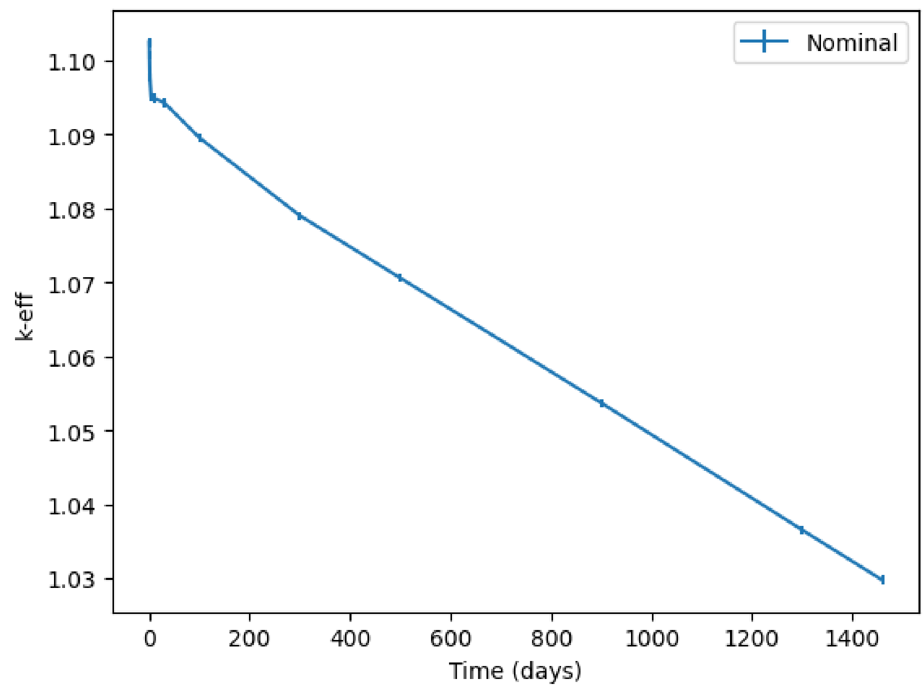


Figure 4: Effective multiplication factor vs. time for the rHPMR at 1000 K. Error bars indicate three-sigma uncertainty.

the configuration discussed in Section 2, while the second is a diversion/misuse case where some of the enriched $UO_2$ TRISO kernels are replaced with $UO_2$ kernels containing roughly natural uranium. In this case, the fuel diverted from the core could have been used for clandestine purposes, where the natural uranium could have been used in an attempt to generate plutonium. Either way, the problem was formulated to showcase the capability not to examine a specific diversion/misuse scenario in-depth. The isotopics for the base case and the natural uranium case are shown in Table 5. Five fuel compacts in the the assembly location, indicated with the red hexagon in Figure 5, were replaced with compacts containing depleted uranium. For clarity, the moderator surrounding the fuel compacts was changed to red to distinguish the two dummy compacts; the graphite material was consistent between the two.

The fuel compacts with naturally enriched TRISO kernels were specifically placed near the center of the core to elicit a statistically significant change in the effective multiplication factor between the two models. Despite this, Table 6 shows the multiplication factors ($k_{eff}$) are within a three-sigma uncertainty of each other. This would likely indicate that startup testing would not be able to discern the two cases, as the control drum angles would likely have significant overlap.

Table 5: Modifications in TRISO fuel kernel composition to simulate diversion case.

| TRISO Kernel Isotope | Base Comp. (atoms/barn-cm) | Diversion Comp. (atoms/barn-cm) |
|---|---|---|
| $U_{238}$ | 4.84171E+21 | 1.72007e+20 |
| $U_{235}$ | 1.93846E+22 | 1.95566e+22 |
| $O_{16}$ | 4.83214E+22 | 4.83214E+22 |
| $O_{17}$ | 1.95625E+19 | 1.95625E+19 |
| $O_{18}$ | 1.11743E+20 | 1.11743E+20 |

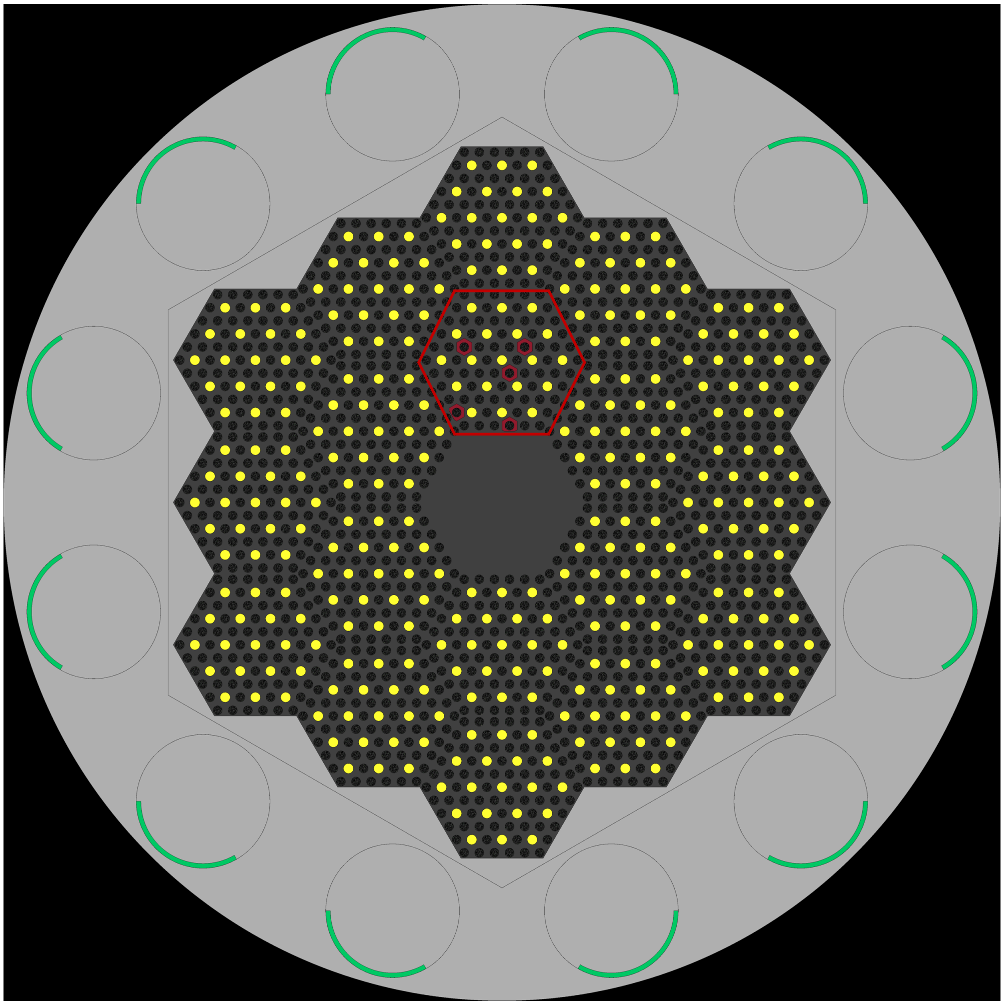

Figure 5: rHPMR radial core layout showing the manipulated fuel assembly indicated with a red hexagon. Five fuel compacts were replaced with the dummy case composition shown in Table 5.

Table 6: Multiplication factor comparison between nominal and diversion scenario.

| Scenario | $k_{eff}$ (std. dev) |
|---|---|
| Nominal | 1.10246 (0.00022) |
| Diversion | 1.10112 (0.00019) |

This trend continues and is highlighted in Figure 6. Over the nearly 4 years of operations, the difference in multiplications factor between the base case and the diversion case remains consistent, in the order of 100 pcm. Due to the small difference between the two curves, it is hypothesized that small perturbations in the compositions will be difficult to detect unless a much larger number of compacts are used for diversion purposes. However, it is noticeable that due to the nature of the fuel form, large quantities of fissile materials cannot be produced in the context of this type of diversion scenario. Given that the multiplication factor is not measured during operations, this would have to translate to changes in the control drum rotation. It is unlikely, but must be verified, that this change would be noticeable in the overall control drum rotation during operations.

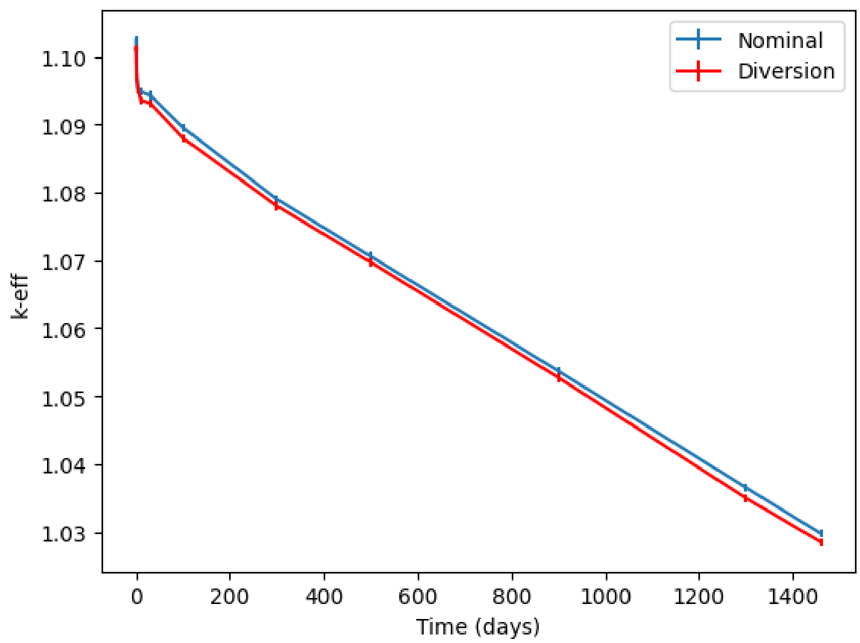


Figure 6: Effective multiplication factor vs. time for the rHPMR at 1000 K for a nominal (blue) and diversion scenario (red). Error bars indicate three-sigma uncertainty.

Figure 7 examines the fission source and thermal flux profiles for the nominal and diversion scenarios. From a qualitative examination of Figure 7, significant changes in fission source and thermal flux can be noticed in the pins containing natural uranium (highlighted with white circles) compared to the nominal kernels. This indicates that additional instrumentation resolving pin-wise power deposition may be necessary to uncover diversion scenarios in which local changes in fuel composition are leveraged to breed Pu-239 or divert U-235.

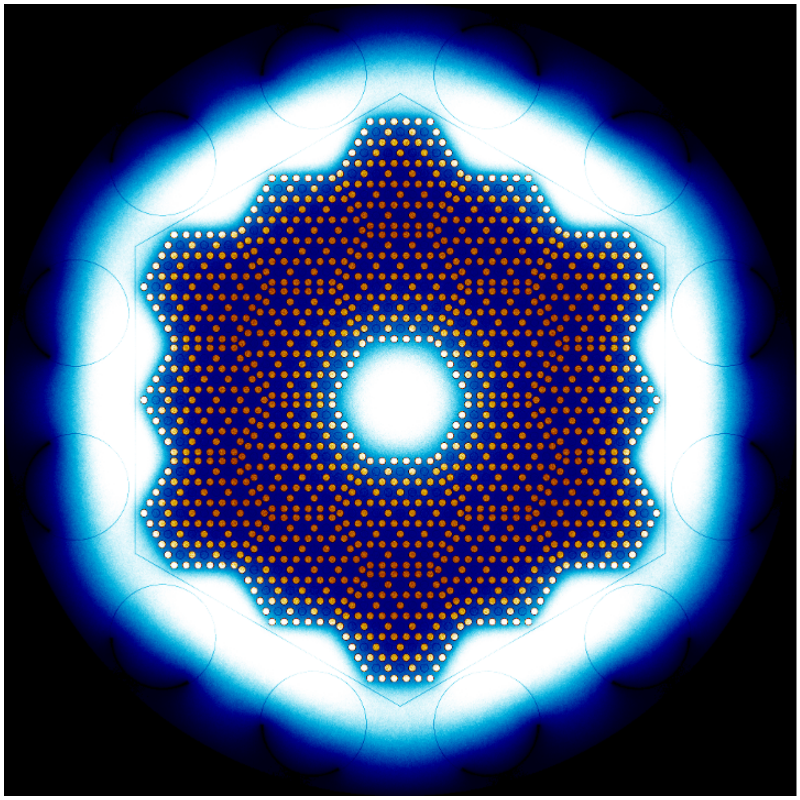

(a) Fission source and thermal flux profile for nominal core.

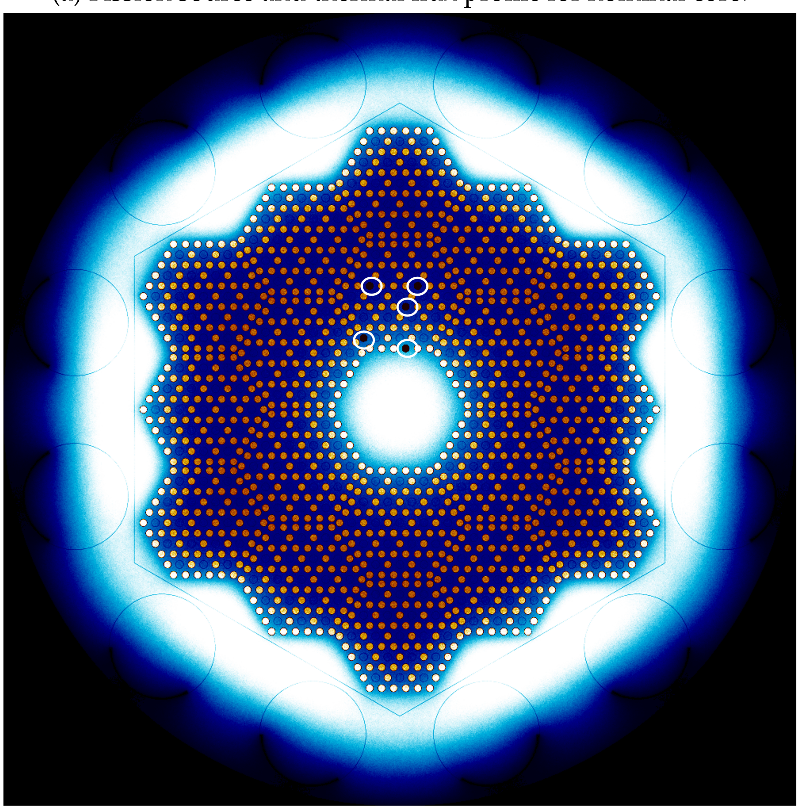

(b) Fission source and thermal flux profile for diversion core.

Figure 7: Fission source (warm colors) and thermal flux (cool colors) distributions for nominal and diversion scenarios for rHPMR.

# 5. DEVELOPMENT OF PRELIMINARY ACQUISITION PATHWAYS

The use of PyRATES enables analysts to easily generate rHPMR configurations corresponding to different acquisition pathway scenarios. This allows the reactor physics team to work closely with the safeguards and machine learning teams to determine potential acquisition pathways.

Table 7 provides selected misuse and diversion scenarios for an HPMR. The first column reports the controllable operational feature that can be manipulated to create fuel misuse and diversion. The second column describes the acquisition scenario deriving from the manipulation of the parameters reported in the first column. The last column deals with quantities that can be used to detect such acquisition pathway. These scenarios are currently envisioned to be analyzed by using the PyRATES-Serpent workflow that was described in Section 3. Current efforts are devoted to exploring additional acquisition pathways that will be used to supplement the ones reported in Table 7 and will be included in the next progress report.

Table 7: Expected parameters of importance related to the high-fidelity neutronics model. The first column provides model parameters that can be perturbed. The second column describes how the model parameter would affect core operations. The third column provides a list of expected detectable signals that would be effected.

| Model Parameter | Scenario Description | Detectable Signals |
|---|---|---|
| TRISO Packing Fraction | The packing fraction can be varied throughout the core to obtain reactor location with higher breeding ratio. In particular, zones with higher fast neutron flux will favor neutron capture by U-238 in lieu of U-235 fission, therefore leading to increased Pu-239 local concentration compared to the average fuel compact. | Local flux distribution, control drum angle, heat pipe temperatures, cycle length |
| Control Drum Rotation Angle Uncertainty | Control drums insertion angle can strongly impact the neutron spectrum in the core periphery, thus enabling the creation of zones with harder neutron spectrum and an environment that is more favorable for Pu-239 breeding. Additionally, small variation in control drums insertion angle aimed at masking a mismatch between the declared core characteristics vs. the actual configuration may be used to conceal diversion scenarios like the one described in Section 4.2. | Local flux distribution, isotopic composition at cycle length |
| Operational Power | MRs can be operated at full power continuously or reduced in power to load-follow. However, lower power could be derived from an intentional manipulation aimed at conserving reactor lifetime despite changes in fuel composition. | Integral power output, isotopic composition at cycle length, control drum angles |
| Fuel Compact Materials | If fuel compacts were removed for diversion, new materials would need to be placed in the core. These materials could be used to manipulate the flux in the reactor to mirror declared operations. This could include adding moderating material to increase reactivity or burnable neutron poisons to suppress the flux. The strategic placement of these material may lead to limited changes in control drum rotation or power changes. | Local flux distribution, control drum angle, isotopics at cycle length, startup measurements |

# 6. SUMMARY AND FUTURE WORK

This report details the development of a high-fidelity reactor physics model of a rHPMR. The main neutronic characteristics of the rHPMR, including temperature reactivity feedback coefficients, total control drums reactivity worth, and effective multiplication factor as a function of time are described. This provides a baseline from which we compare various diversion and misuse scenarios.

The process of automating the generation of rHPMR models using a Python wrapper for the purpose of simulating APA is also described. This wrapper is used to model and simulate a case of fuel diversion. The rHPMR provides a generic model that researchers can utilize to make safeguards considerations (i.e. perform fundamental safeguards by design analyses) without disclosing proprietary information. In this workscope, the rHPMR benchmark is used to exercise the computational tools later to be utilized for the analysis of the NTR.

The PyRATES-Serpent workflow is then exercised to examine a simplified diversion scenario in which natural uranium is used to divert uranium from the core and create higher local concentration of Pu-239. From the analysis, it is found that due to the local nature of the perturbation, the diversion scenario is not detectable through differences in multiplication factors. However, local flux readings could be used to detect the diversion attempt due to different in fluxes between base case and modified reactor configuration.

Negotiations are currently underway between Westinghouse and INL to obtain design information for the NTR; once the negotiations have been completed, a separate report will be delivered to detail the neutronics characteristics. Future work will be devoted to defining and exploring various acquisition pathways using the PyRATES-Serpent workflow developed here. The same workflow will be used to study the NTR once detailed engineering specifications are obtained from Westinghouse.

# REFERENCES


[1] W. E. Company, “evinci™ microreactor selected for department of energy feeed contract.” Available at https://info.westinghousenuclear.com/news/evinci-microreactor-doe-feeed-contract (2024/04/29).

[2] N. Choi, M. Jaradat, V. Laboure, J. Christensen, and S. Terlizzi, “Advancements in multi-physics microdepletion analysis of an evinci™-like microreactor leveraging openmc-crab workflow,” Tech. Rep. INL/RPT-24-77346, Idaho National Laboratory, 2024.

[3] S. Terlizzi and V. Labouré, “Asymptotic hydrogen redistribution analysis in yttrium-hydride-moderated heat-pipe-cooled microreactors using direwolf,” *Annals of Nuclear Energy*, vol. 186, p. 109735, 2023.

[4] J. D. Stempien, J. D. hunn, R. N. Morris, T. J. Gerczak, and P. A. Demkowicz, “Agr-2 triso fuel post-irradiation examination final report,” Tech. Rep. INL/EXT-21-64279-Rev000, Idaho National Laboratory, 9 2021.

[5] N. Roskoff, V. Kucukboyaci, A. Levinsky, V. M. Laboure, J. R. Harter, A. X. Zabriskie, and L. C. Madeleine Charlot, “Modeling and analysis of a micro-reactor using the direwolf code suite,” (Pittsburgh, PA, United States), International Conference on Physics of Reactors 2022 (PHYSOR 2022), 5 2022.

[6] R. Stewart, P. Balestra, D. Reger, E. Merzari, and G. Strydom, “High-fidelity simulations of the run-in process for a pebble-bed reactor,” *Annals of Nuclear Energy*, vol. 195, p. 110193, 2024.

[7] R. Stewart, A. Shields, C. Pope, J. Darrington, K. Wilsdon, S. Bays, K. Heaps, J. Scott, G. Reyes, M. Schanfein, E. Trevino, J. Palmer, and C. Ritter, “A digital twin of the agn-201 reactor to simulate nuclear proliferation,” in *Proceedings of the INMM/ESARDA 2023 Joint Annual Meeting*, 2023.

[8] J. Leppänen, “Serpent– a continuous-energy Monte Carlo reactor physics burnup calculation code.,” tech. rep., VTT Technical Research Centre of Finland, 2015.

[9] E. R. J. Woodcock and T. C. Longworth, “Techniques used in the gem code for monte carlo neutronics calculations in reactors and other systems of complex geometry,” *ANL-7050 Technical report*, 1965.

[10] M. Chadwick, P. Obložinský, M. Herman, N. Greene, R. McKnight, D. Smith, P. Young, R. MacFarlane, G. Hale, S. Frankle, A. Kahler, T. Kawano, R. Little, D. Madland, P. Moller, R. Mosteller, P. Page, P. Talou, H. Trellue, M. White, W. Wilson, R. Arcilla, C. Dunford, S. Mughabghab, B. Pritychenko, D. Rochman, A. Sonzogni, C. Lubitz, T. Trumbull, J. Weinman, D. Brown, D. Cullen, D. Heinrichs, D. McNabb, H. Derrien, M. Dunn, N. Larson, L. Leal, A. Carlson, R. Block, J. Briggs, E. Cheng, H. Huria, M. Zerkle, K. Kozier, A. Courcelle, V. Pronyaev, and S. van der Marck, “Endf/b-vii.0: Next generation evaluated nuclear data library for nuclear science and technology,” *Nuclear Data Sheets*, vol. 107, no. 12, pp. 2931–3060, 2006. Evaluated Nuclear Data File ENDF/B-VII.0.